EFFECTS OF PANEL ZONE DEFORMATIONS ON CYCLIC PERFORMANCE OF WELDED MOMENT CONNECTIONS

K C LIN[1], K C TSAI[2], S L KONG[3] And SHANG-HSIEN HSIEH[4]

SUMMARY

This paper presents the performance of four full-scale welded beam-to-column subassemblies constructed with RC slabs and weak panel zones under the cyclic loading. The improved connection details proposed by SAC (1995) were adopted in these specimens. Test results indicate that ductile fractures of the beam bottom flange occurred in three of the four specimens. The use of notch-tough welding rods and the improved connection details effectively prevented the brittle fracture occurred in the beam-to-column welds. Experimental results show that the total plastic rotations of all joints exceed 0.03 radian, while the total rotations of the joints range from 0.05 to 0.066 radian. Test results also demonstrate that the panel zones possess excellent inelastic deformation capacity, having the ductility ratios more than 13, even up to 20. Test results confirmed that local kinks developed at beam and column flanges, triggering the ductile fractures of beam or column flanges near these kinks, when large inelastic deformations occurred in the panel zone. It is also found that the shear strength and the elastic stiffness of the panel zone are not linearly proportional to the total thickness of the panel zone including the doubler plate. A tri-linear force versus deformation relationships for panel zone incorporating the elastic stiffness of both the column web and column flange is present. The proposed mechanical model predict the experimental responses accurately

INTRODUCTION

As shown in Fig. 1, a steel beam-to-wide flange column panel zone (PZ) joint consists of both column flanges, top and bottom continuity plates, and the column web in the beam-to-column intersection. In a typical seismic moment resisting frame, the shear of PZ is caused by the unbalanced moment induced by two beam end moments. Both moments M_b and M_c (shown in Fig. 1) primarily caused by the frame lateral forces. It can be assumed that the unbalanced moment ΔM ($=M_b+M_c$) is completely transferred to PZ through the beam flanges. Thus, the shear, V, in a PZ is $V = \Delta M/(d_b - t_{cf}) - V_{Col}$, where V_{Col} is the column shear obtained by considering the moment equilibrium at the center of PZ, d_b and t_{bf} are depth and flange thickness of the beam, respectively. Krawinkler (1978) indicated that the yield shear strength, V_y, of the PZ is [illegible], based on the Von-Mises yield criterion for pure shear state $(\tau_y = F_y/\sqrt{3})$ and assuming the effective shear area of an PZ is $0.95d_ct$. Considering the yield shear strength, V_y, of the PZ and the average shear yield strain of the PZ, γ_y, $(= F_y/(\sqrt{3}G))$ are reached simultaneously, the elastic stiffness of the PZ can be obtained:

$$K_e = \frac{V_y}{\gamma_y} = 0.95d_c tG \quad (1)$$

where d_c is the depth of the column, and G is the shear modulus of the PZ's web. Based on the mechanical model proposed by Krawinkler in 1978, PZ's web is elastic perfect plastic material to offer shear strength before and immediately after PZ yielding. Column flanges' effects on PZ are considered as four springs at the corners of the

[1] *Graduate Research Assistant, Department of Civil Engineering, National Taiwan University, Taipei, Taiwan*
[2] *Professor, Department of Civil Engineering, National Taiwan University, Taipei, Taiwan Email: kctsai@ce.ntu.edu.tw*
[3] *Graduate Research Assistant, Department of Civil Engineering, National Taiwan University, Taipei, Taiwan*
[4] *Associate Professor, Department of Civil Engineering, National Taiwan University, Taipei, Taiwan*

PZ, offering shear strength after PZ yielding. The ultimate shear strength corresponding to the yielding of the column flanges at a deformation of about four times the shear yield strain ($4\gamma_y$) of the PZ is therefore:

$$V_K = 0.55F_y d_c t(1 + \frac{3.45 b_c t_{cf}^2}{d_b d_c t}) \quad (2)$$

where d_b, t_{cf}, and b_c are depth of beam, thickness and width of column flange, respectively. Past research results indicate that the weak PZ can develop significant inelastic strength and deformation (Krawinkler 1978, Popov et al. 1985) after the initial yielding of the PZ. Therefore, in 1988 UBC and up to the most recent version of UBC (1997) for allowable stress design method, the design shear strength of PZ take a simplified form of equation (2) as

$$V_{UBC} = 0.55F_y d_c t(1 + \frac{3 b_c t_{cf}^2}{d_b d_c t}) \quad (3)$$

in which t is the total thickness of the PZ web including the doubler plate. In order to allow the PZ to participate in the inelastic deformation, the upper limit of the design load of the PZ is only 0.8 times the summation of the plastic moments of beams connected to the PZ. Thus, the weak PZ design following the UBC provisions was allowed before, and is still permitted after, the Northridge Earthquake. The objectives of this research are to study the effects of the weak PZ on the overall performance of the beam-to-column joints. Effects of the RC slab and influence of an improved connection detail minimizing the effects of the initial cracks, which are below the beam flanges and caused by the backing bars, on the cyclic performance of joints are also assessed. The force versus deformation relationships of the panel zone are also critically reviewed. Nonlinear finite element analyses are conducted in order to gain insight into these issues. A tri-linear force-deformation model is constructed from the results of testing and finite element analysis.

EXPERIMENTAL PROGRAM

There are four full-scale specimens, CB1 through CB4, in this test program. Each specimen consists of one column and two beams. The experimental setup is shown in Fig. 2. Table 1 and 2 summarize the member sizes and the strengths of all specimens, respectively. The design shear strength of the PZs for all specimens is based on Eq. 3. The design shear demands of PZs are V_{d1} (Specimens CB1 and CB2) and V_{d2} (CB3 and CB4), computed from 1.0 and 0.8 times the sum of two beam plastic moment capacities, respectively. The resulting doubler plate thicknesses are 16, 12 and 6mm for Specimens CB1, CB2 and CB3, respectively. Specimen CB4 does not require the doubler plate. All doubler plates of the specimens are A572 grade 50 steel. The strength factors of specimens are shown in Table 3. The tabulated values are computed from actual material strength. These values indicate that except Specimen CB3 (0.97), all other specimens are slightly under-designed. Nevertheless, the upper bound design load (load factor 0.8) prescribed in the allowable stress design method in UBC (1997) for the PZ has been considered.

The fabrication details of beam-to-column joints are shown in Fig. 3. The doubler plate extends 100-mm above and below the top and bottom continuity plates, and uses two 25-mm diameter equally spaced plug welds to connect the column web. At the perimeter of the doubler plate, complete groove welds are used to joint the column flanges on the left and right edges while using fillet welds to joint the column web on the top and bottom edges. Two 24-mm diameter high strength bolts of F10T grade are used to connect the beam web before the fillet welds are made to attach the beam web to the shear tab (15-mm thick). It should be noted that the improved connection details proposed by SAC (1995) are adopted in these specimens. It requires that the end tabs for the beam top and bottom flange welds be removed and joints be ground smooth. In addition, the backing bar for the beam bottom flange welds be removed. The added fillet welds are made at the underside of the beam bottom flange to column flange joint after arc gauging possible defects at root of the complete groove welds. The backing bar for the beam top flange welds is remained. Finally, the reinforcing fillet welds are made below the top backing bar connecting to column flange. All beam flange welds are made by using the shielded metal arc welding (SMAW) procedures. The electrodes are of E7016 grade with a specified Charpy V-notch impact strength of 20 ft-lb at 0 degree F. All four specimens are constructed with the RC slab using 24Mpa strength concrete over the ALK-08 type of metal deck. The strength of the shear studs between the beam and slab is adequate for the fully composite section specified by AISC ASD (1989). Two rows of 19-mm diameter shear studs at a spacing of 150-mm are installed. The tests are conducted using cyclically increasing displacement control method to drive two vertical actuators placed at the two beam tips. The top and bottom ends of the column are hinge supports. An axial force of 0.17 times the yield axial strength is applied and maintained for all specimens.

TEST RESULTS

Deformation and Fracture CHARACTERISTICS of Beam-to-Column Joints

As shown in Table 5, the plastic rotations of four beam-to-column joints all exceed 0.03 radian. They are contributed completely by the beams and the PZs, columns remain elastic during the test. In addition, all PZs carry more than about 70% of the total plastic rotation of the joints, and all beams do about only 30% or less. As shown in Figs. 4 and 5, test results also confirm that plastic rotational capacity of the beams connected to the weak PZ is reduced as the shear strength of PZ decreases. The failure modes of the specimens contain no brittle fracture of the welds or base metal. Except Specimen CB4, all specimens ductily fractured at both beam bottom flanges near the beam web cope as shown in Fig. 6 after the PZs have developed a very large inelastic deformation. As shown in Fig. 7, Specimen CB4 fractured at the west column flange within the PZ near the joint connected to the beam bottom flange. It is observed that rather severe local kinks occurred at the beam and column flanges close to the four corners of the PZ after large inelastic deformations developed in the PZ. These severe local kinks, similar to those cited by others (Krawinkler 1978), appears to be the key factor causing the aforementioned fractures. Nevertheless, these ductile fractures occurred after a very large plastic rotation developed in the PZ. Thus, the test results seem to suggest that the uses of high impact strength electrode and the improved connection details proposed by SAC (1995) can properly prevent undesirable brittle fracture of the welds or joints. However, since local kinks induced by large PZ deformations seem to cause fractures near the kinks, it appears that the upper bound of the PZ design load of $0.8\Sigma M_P$ specified in UBC 97 should be somewhat raised in order to prevent excessive PZ deformations.

Performance of WEAK Panel Zones

Test results demonstrate that properly detailed panel zones possess excellent inelastic deformation capacity, as shown in Fig. 4 and Table 4. The ultimate shear deformations of four PZs range from 0.04 to 0.067 radian, and the ductility ratios are more than 13 even up to 20. PZs also develop large reserved shear strength after yielding. The PZ maximum shear to yield strength ratios are between 1.78 and 2.05. The reserved shear strengths of PZ are resulted from strain hardening and the strength contributions of continuity plates and column flanges surrounding the PZ. The high ductility and the reserved strength characteristics demonstrate that PZ shear yielding is a stable and excellent energy dissipation mechanism.

Shear yield Strength and Elastic Stiffness of The Panel Zone

Experimental results show that the shear yield strength and elastic stiffness of the PZ are not directly proportional to the total thickness of the PZ joint. It is found that the difference between the theoretical predictions and the experimental results increases as the total PZ thickness (including the doubler plate) increases. The comparisons are shown in Table 6 and 7. The largest discrepancies of the shear yield strength and elastic stiffness are 49% and 31%, respectively. It is noteworthy that these theoretical predictions are rather unconservative for design. Thus, it warrants further studies of this subject. A more accurate trilinear force versus deformation relationships for the PZs have been developed recently (Tsai et al. 1998).

Effects of the RC slab on the stiffness and strength of the beam-to-column joints before yielding is apparent (not shown here). But the effects are negligible especially when the PZs develop large deformations. That is, the difference on beam end plastic moments evaluated for the bare steel beam and the composite beam is small in the design of seismic moment joints.

ANALYTICAL STUDIES

It is evident that the elastic stiffness and the strength can not be satisfactorily predicted by the available mechanical models. Therefore, finite element analyses were conducted in order to gain insights into the force-deformation relationships of the PZ. Observations made from the finite element responses were then used to construct the simplified force-deformation relationships. By integrating the shear stress in the column web, it is found that the column flange should be considered in the approximation of the stiffness and the yield strength before, not just after, the yielding of the entire PZ. A tri-linear force versus deformation relationships of the PZ can be constructed by direct adding the bilinear responses of the column web and the column flanges as shown in Fig. 8. From the finite element analyses, the shear area of the column web is found about equal to the product of the web's thickness and a reduced column depth of d_c-2.3t, where d_c and t are the column depth and the web's thickness, respectively. It is also found that the shear strain at the center of the PZ is significantly greater than that at the four corners, and the entire PZ reaches the significant yield state at a shear deformation of about $1.25\gamma_y$. Therefore, the elastic stiffness of the PZ can be estimated as

$$K_e^* = \left[(d_c - 2.3t)t + \frac{5.53 b_c t_{cf}^3}{d_b^2} \right] G \tag{4}$$

The shear yield strength of the PZ can be approximated as

$$V_y^* = \left[0.577(d_c - 2.3t)t + \frac{3.19 b_c t_{cf}^3}{d_b^2} \right] F_y \tag{5}$$

It is also found that the column flanges reach the elastic limit at a PZ shear deformation of about $4\gamma_y$. Therefore, the PZ shear strength at a deformation of $4\gamma_y$ is

$$V_y^* = \left[0.801(d_c - 2.3t)t + \frac{12.8 b_c t_{cf}^3}{d_b^2} \right] F_y \tag{6}$$

Tables 6 and 7 compare the proposed force-deformation relationships with the experimental elastic stiffness, initial yield and the strength at a shear deformation of $4\gamma_y$. It is evident that the proposed mechanical models predict the experimental responses accurately.

CONCLUSIONS

Based on these tests, several conclusions can be drawn as follows:

1. PZ specimens show excellent shear dissipation characteristics, the largest shear deformation and ductility ratio are 0.065 radian and 20, respectively. In addition, properly detailed beam-to-column joints constructed with the weak PZ can sustain large inelastic deformations. The plastic rotations of all specimens exceed 0.03 radian, even up to 0.056 radian.
2. It is found that the beam plastic rotational capacities of the specimens with the weak PZ are reduced as the PZ shear strength decreases. In addition, severe local kinks may develop at the beam or column flanges as the PZ deformations become excessive. Test results confirm that beam or column flange fracture can occur near these kinks. Therefore, it appears that the upper bound of PZ's design load of $0.8\Sigma M_P$ prescribed in UBC97 should be increased in order to prevent excessive deformations occurred in the PZ. This upper bound design load has been changed to lower bound design load in the Taiwanese building code. In addition, the contribution of the column flanges on the PZ strength has been excluded in the computation of PZ design strength.
3. Based on the failure modes observed, it is apparent that the use of notch-tough electrodes (E7016) and the improved connection details proposed by SAC (1995) effectively prevent the brittle fracture occurred in the beam flange welds.
4. The shear yield strength and the elastic stiffness of the PZ are not linearly proportional to the total thickness of PZ including the doubler plate.
5. The proposed force versus deformation relationships predicted the elastic stiffness and the shear strength of the PZ accurately.

ACKNOWLEDGEMENTS

The authors gratefully acknowledge the support of National Science Council of the Republic of China and the Sinotech Foundation for Research and Development of Engineering and Technology.

REFERENCES

AISC, *Manual of STEEL CONSTRUCTION – Allowable Stress Design*, ninth edition, Chicago, Illinois, (1989).

Krawinkler, H., "Shear in beam-column joints in seismic design of steel frames," *Engineering Journal*, AISC, Vol. 15, No. 2, pp.82-91 (1978).

Popov, E. P., Amin, N. R., Louis, J. J. C. and Stephen, R.M., "Cyclic behavior of large beam-column assemblies," *Earthquake Spectra*, 1, No. 2 (1985).

SAC "Interim guideline – evaluation, repair, modification and design of welded steel moment frame structure," *Report No. SAC-95-02*, SAC Joint Venture, CA, FEMA 267 (1995).

Tsai, K. C., Kong, S. L., and Lin, K. C., "Experimental behavior of beam-column panel zone joints undergo large shear deformation," *Report No. NCREE 98-014*, NCREE, 1998. (in Chinese)

UBC, *Uniform Building Code*, International Conference of Building Officials, Whittier, CA (1994, 1997).

Table 1 Material and size of specimens

Beam (Rolled Shape)			
Web		Flange	
F_y(MPa)	F_u(MPa)	F_y(MPa)	F_u(MPa)
387.2 [a]	456.9 [a]	307.8 [a]	456.4 [a]
364.5 [b]	463.6 [b]	293.1 [b]	449.5 [b]
Column (Bulit-up)			
Web		Flange	
F_y(MPa)	F_u(MPa)	F_y(MPa)	F_u(MPa)
425.9	578.7	426.2 [c]	538.3 [c]
425.9	578.7	411.6 [d]	584.3 [d]

Doubler Plate		
Thickness	F_y(MPa)	F_u(MPa)
6mm	432.9	528.4
12mm	413.8	532.3
16mm	414.2	565.7

Concrete:	
F_c'=7.35(MPa) [a]	F_c'=9.62(MPa) [b]

[a] ? for Specimens CB1 & CB2.
[b] ? for Specimens CB3 & CB4.
[c] ? for Specimens CB1 & CB3.
[d] ? for Specimens CB2 & CB4.

Table 3 Design factors of panel zone specimens

Spec.	M_p (kN-m)	V_{d1} (kN)	V_{d2} (kN)	V_y (kN)	V_{UBC} (kN)	$\frac{V_{d1}}{V_y}$	$\frac{V_{d1}}{V_{UBC}}$	$\frac{V_{d2}}{V_y}$	$\frac{V_{d2}}{V_{UBC}}$
CB1	881	2508	2006	2249	2465	1.11	1.02	0.89	0.81
CB2	881	2508	2006	1968	2395	1.27	1.05	1.02	0.84
CB3	614	2180	1744	1546	1807	1.41	1.21	1.13	0.97
CB4	614	2180	1744	1124	1639	1.94	1.33	1.55	1.06

V_{d1} $=\Sigma M_p(1/0.95d_b-L/(L-d_c)/H)$

V_{d2} $=0.8\Sigma M_p(1/0.95d_b-L/(L-d_c)/H)$

V_y $= 0.55F_yd_ct$

$V_{u,Code}$ $= 0.55F_yd_ct(1+3b_ct_{cf}^2/d_bd_ct)$

Table 4 Test results of panel zone shear strength and deformation

Spec.	? u (%rad)	? y (%rad)	$\frac{\gamma_u}{\gamma_y}$	$V_{u,exp}$ (kN)	$V_{max,exp}$ (kN)	$V_{y,exp}$ (kN)	$\frac{V_{u,exp}}{V_{y,exp}}$	$\frac{V_{max,exp}}{V_{y,exp}}$
CB1	4.02	0.32	12.6	2734	2956	1513	1.81	1.95
CB2	4.21	0.32	13.1	2465	2802	1395	1.77	2.01
CB3	5.91	0.32	18.5	2413	2405	1350	1.79	1.78
CB4	6.77	0.32	21.2	1923	2042	995	1.93	2.05

$\gamma_{u,exp}$: Experimental ultimate PZ shear deformation
γ_y : Theoretical PZ shear yield deformation
$V_{u,exp}$: Experimental ultimate shear force of PZ
$V_{max,exp}$: Experimental maximum ultimate shear force of PZ

Table 5 Total and component plastic rotations of specimens

Specimen			γ^{P}_{PZ} (%rad)	θ^{P}_{Total} (%rad)	θ^{P}_{PZ} (%rad)	θ^{P}_{Beam} (%rad)	$\frac{\theta^{P}_{Total}}{\theta_{Total}}$ (%)	$\frac{\theta^{P}_{PZ}}{\theta^{P}_{Total}}$ (%)	$\frac{\theta^{P}_{Beam}}{\theta^{P}_{Total}}$ (%)
CB1	E	+	3.41	3.83	2.57	1.26	77.4	67.1	32.9
		-	3.16	3.55	2.38	1.17	71.1	67.0	33.0
	W	+	3.39	3.56	2.55	1.01	72.0	71.6	28.4
		-	3.22	3.11	2.43	0.68	62.2	78.1	21.9
CB2	E	+	3.86	3.98	2.91	1.07	80.4	73.1	26.9
		-	3.25	3.47	2.44	1.03	69.6	70.3	29.7
	W	+	3.37	3.78	2.54	1.24	76.2	67.2	32.8
		-	3.69	3.34	2.78	0.56	66.8	83.2	16.8
CB3	E	+	5.57	5.27	4.37	0.90	80.1	82.9	17.1
		-	5.25	5.21	4.12	1.09	79.2	79.1	20.9
	W	+	4.83	4.85	3.79	1.06	73.9	78.1	21.9
		-	5.65	5.36	4.43	0.93	81.7	82.6	17.4
CB4	E	+	5.69	5.42	4.46	0.96	81.9	82.3	17.7
		-	5.90	5.44	4.62	0.82	83.5	84.9	15.1
	W	+	6.03	5.60	4.73	0.87	84.2	84.5	15.5
		-	5.65	5.44	4.43	1.01	83.0	81.4	18.6

Table 6 Experimental shear yield strength of panel zone

Spec.	$K_{e,K}$ (MN/rad)	K^{*}_{e} (MN/rad)	$K_{e,exp}$ (MN/rad)	$\frac{K_{e,K}}{K_{e,exp}}$	$\frac{K^{*}_{e}}{K_{e,exp}}$
CB1	703	563	535	1.31	1.05
CB2	614	523	506	1.21	1.03
CB3	483	434	448	1.08	0.97
CB4	351	346	352	1.00	0.98

Table 7 Experimental elastic stiffness of panel zone

Spec.	$V_{y,K}$ (kN)	V^{*}_{y} (kN)	$V_{y,exp}$ (kN)	$\frac{V_{y,K}}{V_{y,exp}}$	$\frac{V^{*}_{y}}{V_{y,exp}}$
CB1	2249	1803	1513	1.49	1.19
CB2	1966	1674	1395	1.41	1.20
CB3	1545	1378	1350	1.14	1.02
CB4	1124	1108	995	1.13	1.11

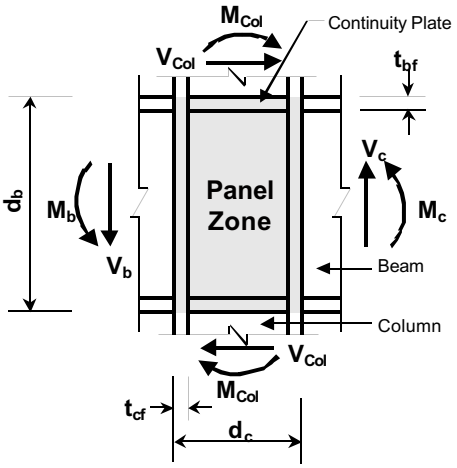

Fig. 1 Distribution of forces in panel zone

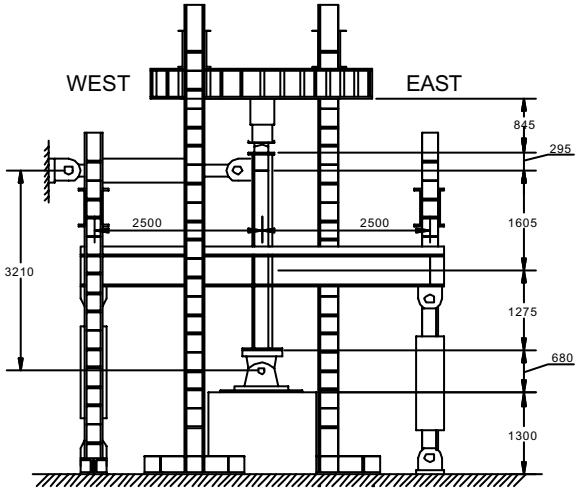

Fig. 2 Experimental setup

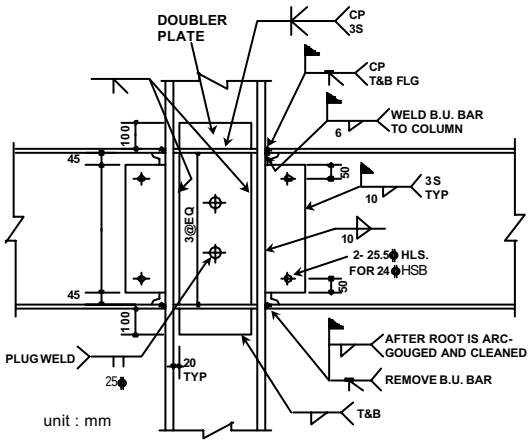

Fig. 3 Details of beam-to-column joint

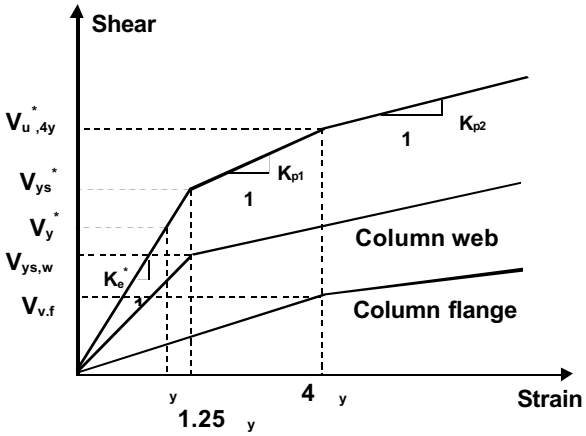

Fig. 8 Tri-linear mechanical model of panel zone

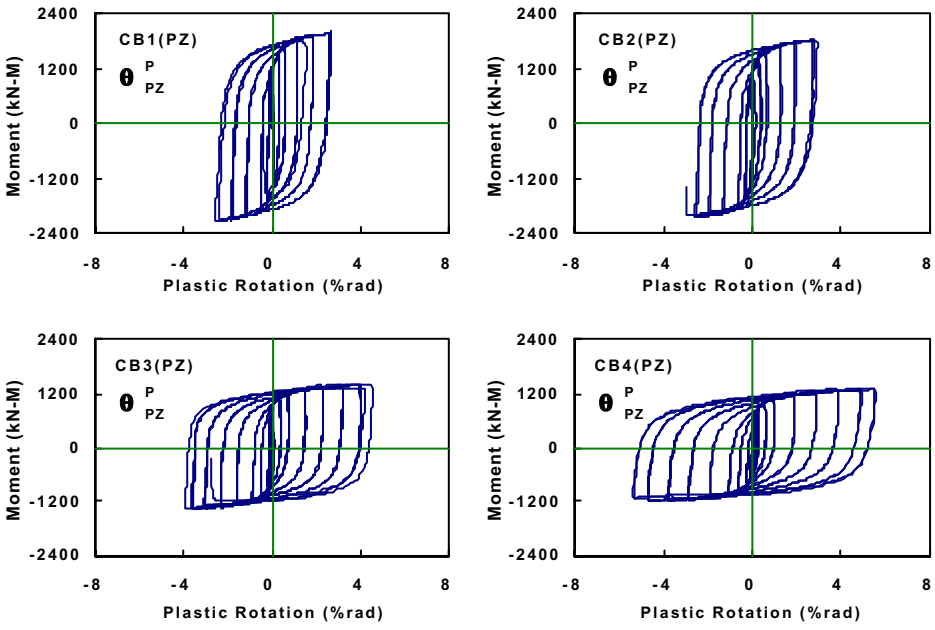

Fig. 4 Cyclic force versus panel zone plastic rotation relationships

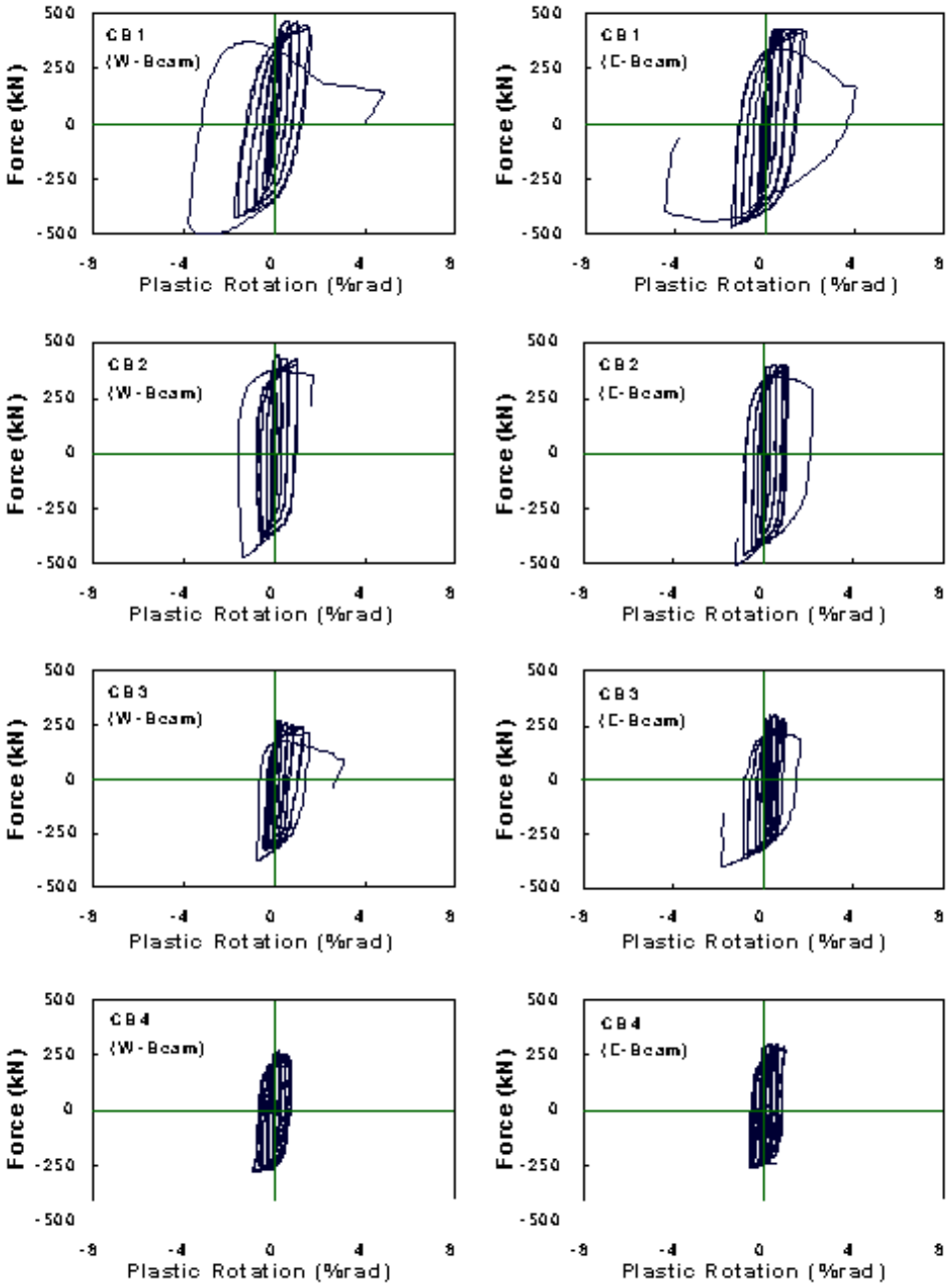

Fig. 5 Cyclic force versus beam plastic rotation relationships

Fig. 6 Typical beam bottom flange fractured near the beam web cope

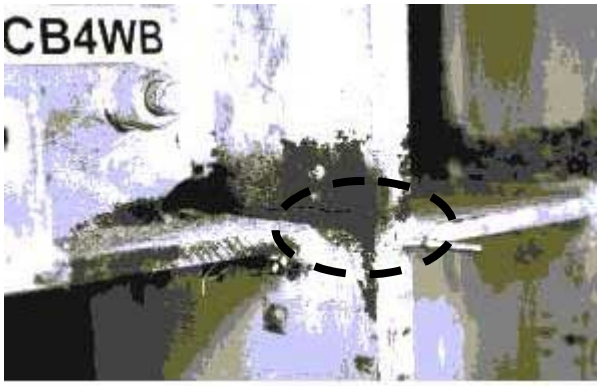

Fig. 7 Column flange fractured at the local kink near the corner of panel zone (CB4)